Forest Ecology and Management 282 (2012) 53–62

Contents lists available at SciVerse ScienceDirect

Forest Ecology and Management

journal homepage: www.elsevier.com/locate/foreco

A distance limited method for sampling downed coarse woody debris

Jeffrey H. Gove [a,*], Mark J. Ducey [b], Harry T. Valentine [a], Michael S. Williams [c]

[a] USDA Forest Service, Northern Research Station, 271 Mast Road, Durham, NH 03824, USA
[b] Department of Natural Resources and the Environment, James Hall, University of New Hampshire, Durham, NH 03824, USA
[c] Risk Assessment and Residue Division, Food Safety Inspection Service, 2150 Centre Ave., Building D, Room 3207, Fort Collins, CO 80526, USA

ARTICLE INFO

Article history:
Received 2 April 2012
Received in revised form 11 June 2012
Accepted 12 June 2012
Available online 26 July 2012

Keywords:
Dead wood
Ecological inventory
Forest inventory
Variable probability sampling

ABSTRACT

A new sampling method for down coarse woody debris is proposed based on limiting the perpendicular distance from individual pieces to a randomly chosen sample point. Two approaches are presented that allow different protocols to be used to determine field measurements; estimators for each protocol are also developed. Both protocols are compared via simulation against existing sampling methods that are closely related in terms of theory and field implementation. The new method performed well in comparison to both fixed-area plot and perpendicular distance sampling, and may provide some simplifications in operational field use.

Published by Elsevier B.V.

1. Introduction

Down coarse woody debris (CWD) plays a number of roles in forest ecosystems. For example, the abundance of CWD is associated with the abundance and diversity of fungi (Pouska et al., 2010) and vertebrates (Bowman et al., 2000; Bunnell and Houde, 2010), and the survival rate of tree seedlings (Harmon and Franklin, 1989). Coarse woody debris is a contributing fuel for stand-regenerating wildfires (van Wagner, 1968), and a dynamic component of an ecosystem's net carbon exchange with the atmosphere. For these and other reasons, sampling strategies for coarse woody debris are employed for a variety of purposes ranging from narrowly focused scientific inquiries to monitoring national forest carbon stocks (Woodall et al., 2008; Woodall et al., 2009). Therefore, it is becoming more important to have sampling methods for down CWD that are easily understood, conveniently applied in the field, and competitive in terms of both time and estimator efficiency with other extant methods.

By convention, a piece of downed CWD is called a log, and a population of CWD may comprise all the logs within some delimited area of a landscape. Common strategies for sampling logs on a landscape include the use of fixed-area plots (Gove and Van Deusen, 2011) or line intersect sampling (LIS) (Warren and Olsen, 1964). Within the last 15 years, several alternative strategies have been advanced that utilize sampling with probability proportional to the size (PPS) of a particular log attribute, for example, length (Ståhl, 1998; Gove and Van Deusen, 2011), length-square (Gove et al., 1999), or midpoint cross-sectional area (Bebber and Thomas, 2003). The PPS method is advantageous because the aggregate amount of the design attribute across the landscape can often be unbiasedly estimated from the count of logs in a sample.

Perpendicular distance sampling (PDS), which was advanced by Williams and Gove, 2003, is remarkable because it samples logs with probability proportional to volume. Consequently, the aggregate volume of the logs on a landscape obtains from counts of logs at sample points. This method also is useful for estimating carbon stocks (Valentine et al., 2008), though one must subsample logs to obtain the carbon to volume ratio. Another closely related method, line intersect distance sampling, combines the strengths of PDS for volume estimation, with the transect protocol of LIS (Affleck, 2008).

Perpendicular distance sampling is so-named because a log is selected into a sample if (i) a line from a sample point intersects the central axis (often termed the 'needle') of a log at a right angle, and (ii) the length of this line is less than some limiting distance, which changes along the log length in a manner that is based on the design attribute (e.g., volume). Design-unbiased protocols for PDS have also been developed for attributes other than volume (e.g., coverage area), and Ducey et al. (2008) have shown how the method can be extended to estimate other attributes. These PDS protocols and others have recently been reviewed and compared by Gove et al. (in press). In this paper, we introduce a strategy for sampling CWD, called distance limited sampling (DLS), which also uses a selection protocol based on a fixed perpendicular

* Corresponding author. Tel.: +1 603 868 7667; fax: +1 603 868 7604.
E-mail addresses: jgove@fs.fed.us (J.H. Gove), mjducey@unh.edu (M.J. Ducey), hvalentine@fs.fed.us (H.T. Valentine), Mike.Williams@fsis.usda.gov (M.S. Williams).

0378-1127/$ - see front matter Published by Elsevier B.V.
http://dx.doi.org/10.1016/j.foreco.2012.06.014

distance—but one that does not vary with log shape as in PDS. The strategy is easy to understand, convenient to apply in the field, and efficient in terms of time and precision.

Distance limited sampling involves sampling with probability proportional to log length, so the aggregate length of logs on the landscape is estimated from the count of logs in the sample. Design-unbiased estimation of other attributes, for example aggregate coverage area or volume obtains, respectively, from either (i) measurement of log coverage area or volume and Horvitz–Thompson estimation, or (ii) measurement of log diameter or cross-sectional area and estimation by Monte Carlo integration. In what follows, we make the distinction between how a log is selected into the sample (the sampling protocol) and how measurements are taken on a log, which in turn determines the estimator to be employed in the expansion of the measurements for the final estimate (the measurement protocol). A log is selected in the same way independent of how the measurements are subsequently taken under this new scheme. But the way the measurements are taken once the log has been included, determines (or is determined by) the estimator used for sample expansion. In the following sections, we describe the protocols and estimation procedures for DLS in detail, and compare the performance of DLS against two competing methods—PDS and the 'sausage' sampling fixed-area plot protocol (Gove and Van Deusen, 2011)—by simulation. Finally, a set of Monte Carlo experiments are conducted to provide a comparative example of the sample size requirements for nominal 95% normal theory confidence interval coverage.

2. Methods

In general, an areal sampling method may be defined through a clear exposition of the probabilistic component of the field sampling selection protocol. This protocol determines the constraints under which a log is sampled through the definition of an object's inclusion zone—that area within which a random point can fall, selecting the object into the sample tally on a given point. This simple formula applies to all areal sampling methods whether they involve lines, fixed-area plots, or variable sized plots. For example, the inclusion zone for an object under line intersect sampling has a well-defined area determined by the line orientation and length, and the shape of the particle being sampled; while the sample point is normally associated with the center point of the line. Similarly, several protocols associated with fixed-area plot methods for down CWD have recently been described by Gove and Van Deusen (2011).

In the following, we assume that the logs lie on a tract $\mathcal{A}$ with area $|\mathcal{A}|$. Furthermore, no restrictions are made with respect to the spatial distribution of the logs in $\mathcal{A}$. Other components of the field protocol, such as the establishment of what constitutes a log in terms of size constraints and structural integrity are part of the design of individual surveys, and are based on the survey objectives; these are not required here for the probabilistic development of the inclusion zone and associated estimators.

2.1. The sampling protocol

The development of the inclusion zone requires the establishment of a log's 'needle' for reference. For intact straight logs, the needle would correspond to the pith along the main axis. For logs that are branched, an imaginary needle can be establish extending from the base to the portion of the most distal branch that still meets the definition of CWD under the survey protocol (Williams et al., 2005). Selection from a given sample point is based on the idea that a log is sampled when the sample point falls perpendicular to the log's needle. The perpendicular distance within which a sample point qualifies on either side of the log is limited, and is denoted D_l. This very simple concept produces a rectangular region with two sides tangent to the log ends, and the other two sides parallel to the log needle as shown in Fig. 1. The area of the zone is $a_i = 2D_lL_i$, where L_i is the length of the ith log. The inclusion probability for a random point sampling the ith log follows simply as

$$\pi_i = \frac{a_i}{|\mathcal{A}|} = \frac{2D_lL_i}{|\mathcal{A}|} \tag{1}$$

It is clear then that both the inclusion area and the inclusion probability differs for each log due to differing log lengths. Thus, the new method is a variable probability method where logs are sampled with probability proportional to their lengths. Fig. 1 also depicts a sample point and perpendicular intersecting the log's needle demonstrating the sample selection concept: since the sample point falls a distance less than D_l from the needle, the log is selected on that point.

2.2. Estimation

The general estimator for variable probability sampling is the Horvitz–Thompson (HT) estimator (Gregoire and Valentine, 2008, p. 215; Thompson, 1992, p. 49). Assume that we want to estimate some attribute y on the population of down logs. Then the HT estimator for the jth sample point is

$$\widehat{Y}_j = \sum_{i=1}^{n_j} \frac{y_i}{\pi_i} \tag{2}$$

where n_j is the number of logs sampled on the jth point. Moreover, if m points are sampled within $\mathcal{A}$, then the mean is given as

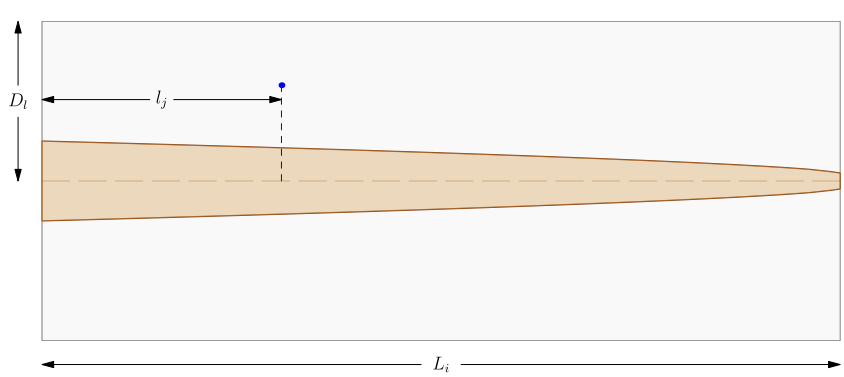

Fig. 1. The inclusion zone for a log with length L_i based on a distance limit of D_l is depicted. The length l_j determined by a random sample point intersecting perpendicular (short dash) with the log's 'needle' (long dash) is also shown.

$$\widehat{\widehat{Y}} = \frac{1}{m}\sum_{j=1}^{m}\widehat{Y}_j \tag{3}$$

with associated unbiased variance estimator

$$\widehat{\mathrm{Var}}(\widehat{\widehat{Y}}) = \frac{1}{m(m-1)}\sum_{j=1}^{m}(\widehat{Y}_j - \widehat{\widehat{Y}})^2 \tag{4}$$

With respect to our distance limited variable length plot method, substituting (1) the estimator (2) becomes

$$\widehat{Y}_j = \frac{|\mathcal{A}|}{2D_l}\sum_{i=1}^{n_j}\frac{y_i}{L_i}$$

or, for m sample points using (3)

$$\widehat{\widehat{Y}} = \frac{|\mathcal{A}|}{2D_l m}\sum_{j=1}^{m}\sum_{i=1}^{n_j}\frac{y_i}{L_i} \tag{5}$$

If the attribute of interest is log length, then $y_i = L_i$ in the above, and a simple count of the logs selected on the sample point will provide an estimate of aggregate length. Other attributes require measurements. For example, volume models such as Smalian's formula (Fraver et al., 2007) can be used to estimate log volume, and in general require measurement of not only log length, but in the case of Smalian's, both end diameters as well. However, if volume from Smalian's is used for y_i in (5), then length again cancels and only the diameter measurements are required. Log density per unit area ($y_i = 1$) requires measurement of log length for each log. Woody biomass can be estimated from the log volume and an estimate of the bulk density, ρ, for the log, either based on an overall species factor or from subsampling (Valentine et al., 2008), and should ideally reflect decay status. Carbon content can similarly be estimated from biomass using a standard conversion of approximately one half, but which may differ by species. Attributes like surface area and coverage area are more problematic and would likely involve a taper model for estimation. The sampling and associated measurement protocols outlined thus far will be referred to as simple distance limited sampling (DLS).

2.2.1. Crude Monte Carlo

In the last section we presented the basic DLS estimator and showed how several quantities, y_i, could be estimated using a protocol that is familiar from other methods. In particular, log volume can be estimated using a model. An alternative protocol to this approach can be developed by considering a subsample within each log for the estimation of volume and other attributes. The subsampling procedure is based on the crude Monte Carlo (CMC) method (Rubinstein and Kroese, 2008, p. 27), which was formalized for forest sampling problems by Valentine et al. (2001). The motivation for using CMC lies in the estimation of integral quantities. For example, suppose we wish to estimate the integral

$$\theta = \int_a^b g(x)\ \mathrm{d}x \tag{6}$$

for some arbitrary function $g(x)$. In CMC, this integral can be estimated using Monte Carlo simulation.

Recall that if the random variable $X \sim f(x)$, then we can write the expectation

$$\mathrm{E}[g(X)] = \int_{-\infty}^{\infty} g(x)f(x)\ \mathrm{d}x \tag{7}$$

Now let $f(x)$ be a uniform distribution on $[a,b]$ such that $X \sim U(a,b)$. Then under the uniform assumption, the integral (6) can be expressed as

$$\begin{aligned}\theta &= \int_a^b g(x)\ \mathrm{d}x = (b-a)\int_a^b g(x)\frac{1}{b-a}\ \mathrm{d}x \\ &= (b-a)\int_a^b g(x)f(x)\ \mathrm{d}x = (b-a)\ \mathrm{E}[g(X)]\end{aligned} \tag{8}$$

where $f(x) = 1/(b-a)$ is the uniform PDF for $X \sim U(a,b)$. The penultimate step in Eq. (8) is in the form of Eq. (7), which yields the final result. The crude Monte Carlo estimator for θ under the uniform assumption is, by (8)

$$\hat{\theta} = \frac{(b-a)}{m}\sum_{j=1}^{m} g(x_j) \tag{9}$$

where m uniform deviates are drawn. This estimator is unbiased and converges to the true θ with probability one by the Strong Law of Large Numbers (Suess and Trumbo, 2010, p. 67). This result can also be arrived at through application of the mean value theorem for integrals (Valentine et al., 2001).

The alternative approach to the direct estimation of log attributes is to consider each an integral quantity in the form (6) to be estimated. For example, log volume can be estimated using (6) where $g(l)$ is cross sectional area, and the limits of integration are from $0 \leqslant l \leqslant L_i$. Table 1 presents several other integral quantities that may easily be verified.

A key observation is that the perpendicular intersection with the ith log's needle from the jth random sample point, determines a random length l_j within the log as illustrated in Fig. 1. Because the sample point is randomly located, the random length l_j so determined is uniformly distributed. Thus, we may write (8) as

$$\theta_i = \int_0^{L_i} g_i(l)\ \mathrm{d}l = L_i\ \mathrm{E}[g_i(L)]$$

which by (9) is estimated as

$$\hat{\theta}_i = \frac{L_i}{m}\sum_{j=1}^{m} g_i(l_j) \tag{10}$$

Letting $y \equiv \theta$ and combining this result with (1) and (2) it is straightforward to show that a design-unbiased estimator for each of the attributes in Table 1 under this distance limited Monte Carlo sampling (DLMCS) protocol is given as

$$\widehat{\widehat{Y}} = \frac{|\mathcal{A}|}{2D_l m}\sum_{j=1}^{m}\sum_{i=1}^{n_j} g_i(l_j) \tag{11}$$

Note in this estimator that selection of the ith log on more than one sample point establishing different random lengths l_j is allowed for. In addition, note that the determination of log length is unnecessary for any integral quantities other than density (Table 1).

Table 1
Integral quantities that can be easily estimated under crude Monte Carlo.

Attribute	$g(l)$	Integral	Integrand and Constant description
Density	$\frac{1}{L}$	$\int_0^L \frac{1}{L}\ \mathrm{d}l = 1$	L is total log length (m)
Length	1	$\int_0^L \mathrm{d}l = L$	
Surface area[a]	$c(l)$	$\int_0^L c(l)\ \mathrm{d}l = a_s$	c is circumference (m)
Coverage area	$d(l)$	$\int_0^L d(l)\ \mathrm{d}l = a_c$	d is diameter (m) parallel to the horizontal plane of the ground
Volume	$x(l)$	$\int_0^L x(l)\ \mathrm{d}l = v$	x is cross sectional area (m^2)
Biomass	$\rho x(l)$	$\rho\int_0^L x(l)\ \mathrm{d}l = y_b$	ρ is bulk density (mass per unit volume)
Carbon	$\psi\rho x(l)$	$\psi\rho\int_0^L x(l)\ \mathrm{d}l = y_c$	ψ biomass to carbon conversion (mass C per mass wood)

[a] This integral is approximate, but very close—compare with Table 2.

2.3. Simulation methods

The unbiasedness of the estimators for the two protocols proposed for this new distance limited method is easy to show. However, the properties of the estimators are still unknown with regard to variability, and this will be addressed through simulations. Specifically, we employ a method formalized by Williams (2001a) and Williams (2001b) called sampling surface simulation. This method divides the tract $\mathcal{A}$ into square grid cells of predetermined resolution. The center of each grid cell is taken as a sample point. And the tract area is populated with a collection of logs whose inclusion zones are known, and therefore can be easily mapped. The sampling surface itself is then developed separately for any given attribute and sampling method or protocol (e.g., DLS or DLMCS) as follows. The grid of cells comprise all possible sample points, m, over the tract at the grid resolution used. At each grid cell center a "sample" is taken such that any logs whose inclusion zone contains the grid cell center are included in the sample for that point. Next, the estimator under consideration is applied to the n_j logs in the sample at the jth point yielding the estimate $\widehat{Y}_j$ for that cell. In this way, a variable sampling surface is built up for the tract, where cells that have $n_j > 1$ logs (due to n_j overlapping inclusion zones) get values that are the sum of the expanded attribute for the n_j logs at that point. All background cells with no overlapping inclusion zones are assigned a zero value.

The sampling surface technique is conceptually simple and has several added benefits over other methods, such as simply saturating the tract $\mathcal{A}$ with random points in a pure Monte Carlo experiment. For example, the sampling surface method allows for visual representation and comparison of different methods for a given attribute; this is important because surface roughness is directly related to estimator variance. Protocols or methods that have larger inclusion zones allow the attribute density to be spread over a larger area, decreasing the variance. And methods that have flat attribute surfaces within inclusion zones generally will have less variance than those methods whose surface varies within the individual zones (this is true for individual logs, but for a population of logs the overall result will depend on the juxtapositions of the logs). Again this allows one to obtain a visual assessment of the effect that different inclusion zone shapes and sizes make in regard to estimator variance for the methods being compared. Finally, while the approach sounds computationally intensive, it can be implemented in a very efficient manner by overlaying individual inclusion zones onto the tract and "heaping" the surface by simple summation of the raster cells. In this way, background cells with no inclusion zones are never visited. This approach has been implemented for the sampling methods and attributes discussed here, as well as several others, in the "sampSurf" package (Gove, in press) for the R statistical language (R Development Core Team, 2012).

Finally, once a sampling surface has been created by the methods described above, statistics can be calculated on the surface. In particular, for an unbiased estimator, the surface mean will approximately equal the true attribute total for the logs in the population. In addition, as mentioned above, the variance of the surface can be calculated by

$$\mathrm{Var}(\widehat{Y}) = \frac{1}{(m-1)}\sum_{j=1}^{m}(\widehat{Y}_j - \widehat{\overline{Y}})^2 \tag{12}$$

where the summation over all m points equates to summation over all m cells in the rectangular grid. Likewise an estimate of the surface standard deviation is simply $\mathrm{SD}(\widehat{Y}) = \sqrt{\mathrm{Var}(\widehat{Y})}$. Note in particular that this is not the variance of the mean estimator given in (4). In all cases the statistics will be close but not exact, as with any simulation method. This is because every possible sample point has not been enumerated (there are infinitely many), only every possible point at the given grid cell resolution. So while small percentage "bias" figures will be reported in the results, these will go to zero as the grid cell resolution increases (smaller cells), and does not equate with a biased estimator. Likewise the estimate of the variance will approach the true variance of the estimator for the population under consideration as $m \to \infty$. In past simulation studies, grid cell resolutions on the order of one quarter to one half meter have proven quite reasonable (Williams and Gove, 2003; Gove et al., 2005; Ståhl et al., 2010; Gove and Van Deusen, 2011), therefore we employ half-meter resolution here.

The log population for the simulations was constructed from a simple taper equation (Van Deusen, 1990) given in Table 2. This table also presents closed-form solutions to the corresponding volume, and coverage area equations, while surface area must be numerically integrated. The taper equation can take on a variety of geometric forms from neiloid ($0 < r \leqslant 2$), through conical ($r = 2$), to parabolic ($r > 2$). A population of $N = 50$ logs was generated and this same population was used in each simulation to compare the methods. Random uniform values for the each quantity were drawn from the following ranges: $D_b \in [8,40]$ cm, $D_u \in [0,0.9] \times D_b$, $L \in [1,10]$ m and $r \in [1,10]$ (refer to Table 2 for definitions). Each log was randomly placed within a tract of $|\mathcal{A}| = 1$ ha, which was minimally buffered such that all inclusion zones fit within the tract, insuring that no edge-effect bias was introduced. Finally, each log was given a random orientation angle $\phi_i \in [0,2\pi]$, $i = 1,\ldots,N$.

2.3.1. Efficiency comparisons with other methods

In order to gauge the efficiency of the new estimators (5) and (11), they must be compared against similar methods. The shape of the sampling surface within the inclusion zones comes into play in determining which methods would best be used as standards. The simple DLS method will have constant surfaces for all attributes within individual log inclusion zones. However, the DLMCS protocol will have a variable surface for all attributes that depend on some function of diameter in Table 1; but surfaces for length and density will be constant. Thus, it is prudent to match methods with similar characteristics to these protocols for the comparisons. In addition, to make a fair comparison in terms of estimator efficiency, the sampling effort (number of total grid cells within log inclusion zones, m_e) should be fairly closely matched between the comparative methods. The mechanism for doing this on each method is explained below.

A closely related technique to simple DLS was described as the so-called 'sausage' method for fixed-radius circular plots (Gove and Van Deusen, 2011). The method uses the same measurement

Table 2
Taper equation and associated equations used in the simulations.

Attribute	Equation
Log Taper (m)	$d(l) = D_u + (D_b - D_u)\left(\frac{L-l}{L}\right)^{\frac{2}{r}}$
Volume (m^3)	$v(l) = \frac{\pi}{4}\left[D_u^2 l + L(D_b - D_u)^2 \frac{r}{r+4}\left(1 - \left(1 - \frac{l}{L}\right)^{\frac{r+4}{r}}\right) + 2LD_u(D_b - D_u)\frac{r}{r+2}\left(1 - \left(1 - \frac{l}{L}\right)^{\frac{r+2}{r}}\right)\right]$
Surface Area (m^2)	$S = \pi \int_0^L d(l)\sqrt{1 + \frac{d'(l)^2}{4}}\,\mathrm{d}l$
	$d'(l) = -2\frac{(D_b - D_u)(L-l)^{\frac{2}{r}-1}}{rL^{\frac{2}{r}}}$
Coverage Area (m^2)	$C(l) = \frac{1}{(r+2)L^{\frac{2}{r}}}\left[(r+2)D_u l L^{\frac{2}{r}} + (L-l)^{\frac{2}{r}}((D_u - D_b)rL + (D_b - D_u)lr) + (D_b - D_u)rL^{\frac{(r+2)}{r}}\right]$

Where D_b and D_u are the large- and small-end log diameters and $0 \leqslant l \leqslant L$ is some intermediate length; $d'(l)$ is the derivative term for the surface area integral—all diameters are in the same units as length.

protocols as described above for DLS, and is a probability proportional to length method, so the surfaces within the inclusion zones are constant for all attributes. It adds a half circular plot to each end of the inclusion zone in Fig. 1 making an overall inclusion area $a_s = 2R\,L_i + \pi R^2$, where R is the plot radius and is directly equivalent to the distance limit D_l. To establish a reasonably equivalent sampling effort to that of DLS for a given distance limit, determine the mean log length ($\bar{L}$) in the population and solve the quadratic $\bar{a}_{dls} = 2R\bar{L} + \pi R^2$ for the plot radius where $\bar{a}_{dls}$ is the DLS inclusion zone area associated with $\bar{L}$.

Perpendicular distance sampling (PDS) (Williams and Gove, 2003) will be used as a comparative technique for DLMCS. PDS selects logs with probability proportional to volume, surface area or coverage area depending on the protocol, yielding a design-unbiased estimate for the protocol attribute. Application is limited here to the volume protocol, under which a count of the number of selected logs per point yields an estimate of volume; other attributes can be estimated via a Monte Carlo extension described by Ducey et al. (2008). The inclusion zone for the volume protocol is an inflated version of log taper in terms of cross-sectional area. The inflation factor is known as the K_{pds} factor and has units m^{-1}. Logs are sampled if the perpendicular distance from the sample point to the log is less than xK_{pds}, where x is the cross-sectional area at the perpendicular to the sample point. To find a reasonably equitable K_{pds} factor, determine the average midpoint diameter for the log population ($\bar{D}_{mid}$) and set $K_{pds} = \frac{4D_l}{\pi \bar{D}_{mid}^2}$. Just how close the resulting sampling effort is to D_l with this approximation will depend on the taper variability in the simulated log population and may require small iterative adjustment to get a roughly equivalent number of sample points.

Fig. 2 presents the synthetic log population used in the simulations, along with the inclusion zones for each of the methods discussed above. Recall that only the measurement protocol is different between DLS and DLMCS, they both share the same inclusion zone. In addition, the sausage inclusion zones are narrower to account for the extra area at the ends, while the PDS inclusion zone width will be roughly D_l at the midpoint of the average log. This figure shows the difficulty in establishing an equitable K_{pds} factor because inclusion zone shape under PDS is an inflated version of cross-sectional taper, which varies for each log depending upon the shape parameter r in the taper equation (Table 2); therefore, it is difficult in general to define and 'average' log shape. The inclusion zones for the sausage method, on the other hand, are readily comparable to that of the distance limited methods.

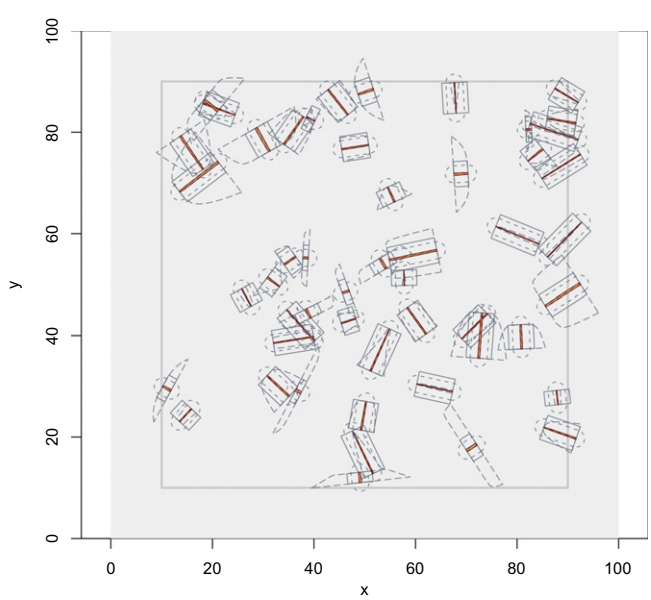

Fig. 2. Population of $N = 50$ logs on a 1 ha tract used in the simulations illustrating the difference between inclusion zones for DLS and DLMCS (solid), PDS (long dash) and sausage (short dash). A distance limit of $D_l = 2.5$ m was used, with corresponding $K_{pds} = 50\ m^{-1}$ and a plot radius of $R = 1.67$ m for the sausage method. A 10 m buffer is also shown.

2.3.2. Sampling distributions and confidence interval estimation

The sampling distribution of the estimators will play a role in determining whether normal theory confidence intervals are appropriate for samples of various sizes recorded in the field. For example, Affleck (2008) questioned whether normal theory or even bootstrap confidence intervals would be appropriate for inferences on the sample mean in moderate sample sizes drawn from simulation results under LIDS, PDS and LIS due to the skewness in the sampling distributions. For normal theory inference to apply, the distribution of sample means drawn from repeated samples of the population sampling distribution for each method must approach a Gaussian distribution by the Central Limit Theorem (Barrett and Nutt, 1979, p. 38). Barrett and Goldsmith (1976) showed that normal theory intervals were applicable for moderately small sample sizes, even in populations with bimodal or negative exponential sampling distributions.

The sampling distribution for a given sampling surface realization by attribute and sampling method is comprised of all possible sample (grid cell) values. A combination of factors actually influences the shape of the sampling distribution, which will differ for each attribute of interest and each sampling method or protocol. First, the methods are all based on PPS sampling theory, and thus are optimized for different attributes: DLS, DLMCS, and sausage for length, and PDS for volume. Second, the measurements taken on the log to estimate a given attribute, especially with DLMCS and PDS, may be quite variable. This last point is related to the form of the estimator itself—compare for example (5) and (11)—and the estimators under PDS for multiple attributes are more irregular then that for DLMCS. The cumulative effect of these factors produces sampling distributions that can vary from quite well behaved to severely multimodal, or negative exponential in shape. As a consequence, the number of samples required for confidence interval estimation will also vary depending on the sampling method and attribute to be estimated.

The goal in this line of investigation is to illustrate these concepts for the simulated population of logs described above, by drawing a simple set of repeated Monte Carlo samples from each sampling surface distribution to determine the normal theory confidence interval coverage rates. The results will be applicable to the population at hand and could be used to establish some general guidelines for determining how large a sample may be required in populations with similar sampling distributions.

3. Results

3.1. Efficiency comparisons with other methods

The results of the simulations for the population of 50 logs are shown in Table 3. Attributes such as surface area, biomass and carbon content are not presented as they are closely related transforms of the variables shown. The first and most important point to notice is that all methods, including the newly proposed DLS and DLMCS are unbiased. These results substantiate our earlier claims concerning the method; the small positive or negative percent bias shown is purely an artifact of sampling, not of the methods themselves as mentioned previously. Approximately $m_e = 4900$ sample points out of $m = 40{,}000$ total cells (roughly 12%) contained samples where logs were recorded because their

Table 3
Results of the simulations for a standard synthetic log population of size $N = 50$ logs. Sampling constants were: $D_l = 2.5$ m, $K_{pds} = 50$ m^{-1}, and $R = 1.67$ m.

Attribute/ protocol	Population total	Sampling surface				
		Estimate	% Bias	SD	Max	m_e[a]
Volume (m^3)						
DLS	13.51	13.50	−0.07	48.50	417	4893
Sausage	13.51	13.54	0.23	47.90	446	4896
DLMCS	13.51	13.51	0.05	49.27	429	4893
PDS	13.51	13.47	−0.27	37.40	300	4927
Length (m)						
DLS	264.04	264.85	0.31	735.1	4000	
Sausage	264.04	264.42	0.15	745.6	4686	
DLMCS	264.04	264.85	0.31	735.1	4000	
PDS	264.04	265.16	0.42	1371.4	82285	
Density						
DLS	50	50.12	0.23	166.9	2002	
Sausage	50	50.14	0.29	148.5	1360	
DLMCS	50	50.12	0.23	166.9	2002	
PDS	50	50.13	0.26	257.2	26229	
Coverage area (m^2)						
DLS	60.50	60.55	0.08	185.7	1423	
Sausage	60.50	60.63	0.22	185.9	1594	
DLMCS	60.50	60.56	0.10	187.1	1456	
PDS	60.50	60.41	−0.15	185.6	3582	

[a] Values for m_e, the number of sampled grid cell centers, are the same for each attribute.

inclusion zones overlapped the grid cell centers for each of the methods. For the two distance limited protocols, the variance (as measured by the standard deviation) was comparable for each attribute with neither protocol showing an advantage. For attributes length and density, the variance was equivalent between these protocols because neither relies on a model or on the CMC approach (Table 1).

The two constant surface methods, DLS and sausage, were also quite similar in their results, and were indistinguishable in terms of variance for volume and coverage area. The sausage method was somewhat better for density, but the opposite was true for length, where DLS had lower variance. However, it is not a good idea to impart too much weight to these rankings with the small synthetic population used in this simulation as the methods will rank somewhat differently under different realizations of the sampling surface from other log populations. The main point is that the two methods are very comparable in their estimation efficacy for each attribute as long as the inclusion zone areas have been equalized on average; they differ mainly in their field protocol. It is interesting to note that because DLS and DLMCS are both similar in result, DLMCS is also comparable to the sausage method.

Among the two variable surface methods, DLMCS and PDS, the rankings are more clear cut for all attributes except coverage area, where they both perform equally well. PDS is optimized for volume, and has a flat sampling surface within individual log inclusion zones for this attribute; thus, it is not surprising that it performs best out of all methods tested for this attribute. This will also be true of biomass and carbon estimates. However, the PDS estimates for length and density are not competitive with the other estimators variance-wise. This has to do with the form of the estimator itself. The estimator for both attributes contains a $x(l_j)^{-1}$ term (see Ducey et al., 2008 for full details); therefore, any log that tapers to a small diameter (or to the tip) will have very small cross-sectional area, causing the estimator to inflate in this area of the stem. In addition, the estimator for log density also includes a L_i^{-1} term, which can be quite variable, but whose magnitude helps assuage the problem. The direct result of this can be seen in the maximum surface values given in Table 3 for PDS. The DLMCS estimator (11) does not suffer from inflation issues due to denominators tending to zero, and is thus a more well-behaved estimator in general for these two quantities.

The maximum height of the sampling surface is closely correlated with the estimator variability ($\mathrm{SD}(\widehat{Y})$); though the comparison is not one-to-one, because the juxtaposition of the logs literally determines how the inclusion zone attribute densities are heaped through summation within overlapping inclusion zones for any synthetic log population. However, it is quite evident that the large variance for length and density under PDS is directly related to the substantially larger peaks in surface height under this method. The results in Table 3 only tell a summary of the full story with regard to differences in the estimators. A more thorough understanding of the various subtleties described above can be seen by examining the resulting sampling surfaces themselves. Because each attribute and method combination results in a different surface, we regard only a subset in what follows.

Figs. 3 and 4 show the resulting sampling surfaces for volume estimation under DLS and DLMCS, respectively. The effect of the estimators is clearly shown in contrasting these two surfaces. First, under DLS, it is clear from the form of the estimator in (5) that y_i is constant for the entire log, for each attribute, and regardless of where the point falls within the inclusion zone. This, therefore, produces the constant surface within individual zones shown. In contrast, the form of the estimator in (11) for DLMCS provides for differing values of $g_i(l_j)$ depending on where the jth sample point lands within the inclusion zone. This produces the variable surface for all quantities but length and density in Table 1. The extent to which the surface slopes is determined by the cross-sectional taper of the log for volume estimation, which can be roughly deduced by the shape of the PDS inclusion zones in Fig. 2, since they are proportional to cross-sectional area. Logs that have little taper in cross-section, will have only gradual slope to the surface, while those that taper more dramatically, have steeper slope. The surface for the sausage method is very similar to that in

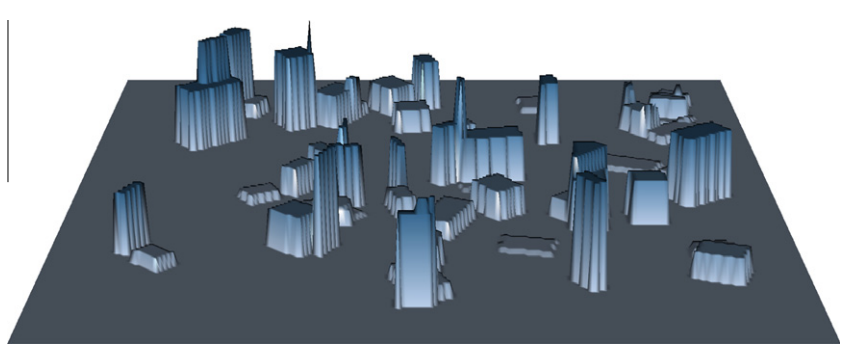

Fig. 3. Sampling surface realization under DLS for volume estimation using the same population of logs as is shown in Fig. 2. The surface is constant within individual log inclusion zones with a maximum of 417 m^3 (Table 3).

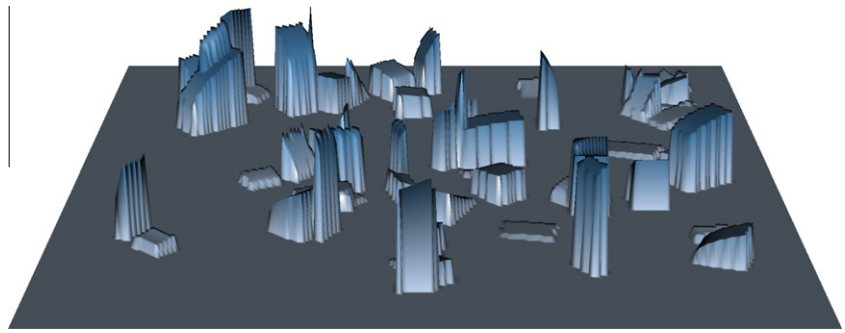

Fig. 4. Sampling surface realization under DLMCS for volume estimation using the same population of logs as is shown in Fig. 2. The surface is variable within individual log inclusion zones with a maximum of 429 m^3 (Table 3).

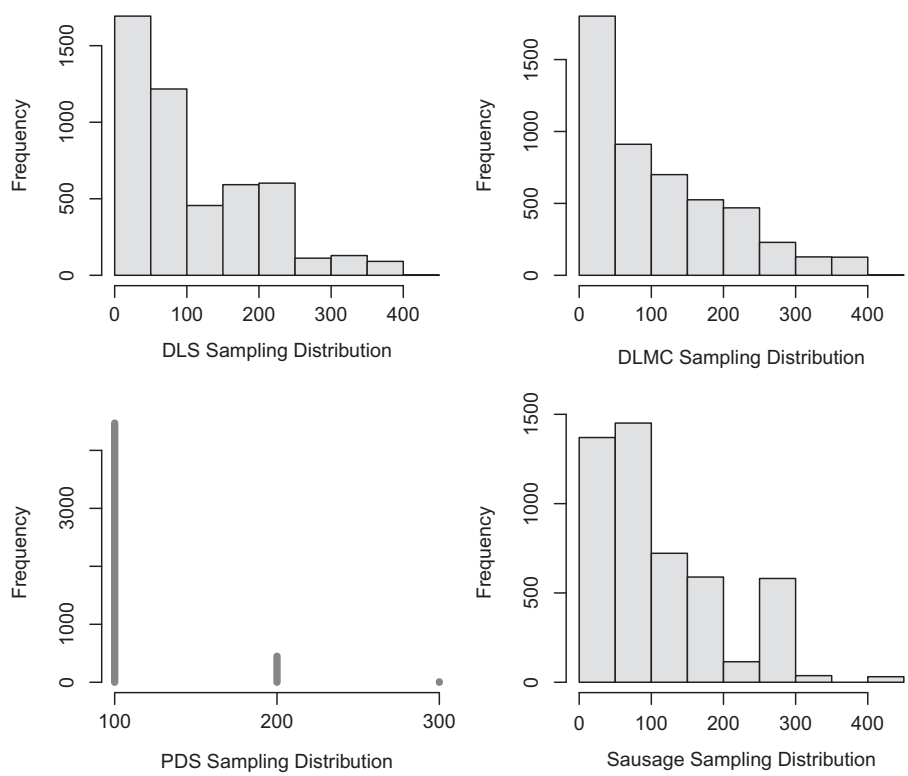

Fig. 5. The zero-truncated sampling distributions of volume for each sampling method based on the sampling surface results in Table 3.

Fig. 3, except the individual zones will be slightly narrower and possess rounded ends. The PDS sampling surface for volume is flat within zones, and has the shape shown for individual logs in Fig. 2. It should be clear that the way the individual zones 'heap' to form the overall surface will be different under each method. Finally, other attributes will also show different results even within methods; for example, PDS for length will be variable, while DLMCS for length will be constant and exactly the same as DLS (Table 1).

3.2. Sampling distributions and confidence interval estimation

As stated previously, the results in this section seek to determine some broad guidelines on how large of a sample is required for nominal 95 percent confidence interval coverage on a population of logs with sampling distributions similar to those described here. The sampling distributions were zero-truncated for the experiment, because while zero is a valid value for a sample point, the number of zero cells is a direct consequence of the tract size and resolution, distance limits, etc., which would make the result conditional on those factors. For example, the sampling distributions for volume are shown in Fig. 5. Note that the distributions vary by method from discretely multimodal (PDS) to mildly exponential.

The results of the confidence interval experiments are presented in Table 4. These results will vary not only with the log population used, but also simply with drawing another set of intervals from the same population in a different Monte Carlo run. Therefore, we consider intervals with approximately 94% coverage to be nominally adequate at the $\alpha = 0.05$ confidence level. The results for volume then suggest that the two distance limited methods would require in the range $20 \leqslant m \leqslant 30$ sample points for interval estimation. Sausage sampling would require perhaps 10–20 more. Interestingly, however, PDS appears to require more than $m = 250$ samples even though it is optimized for volume. The reason is because each log counts for a fixed amount of volume at each sample point, in this case with $K_{pds} = 50$, this translates to 100 m^3 ha^{-1}.

Table 4
Approximate coverage percentages (nominal 95% target coverage) of the population mean for normal theory confidence intervals. The results are based on drawing 1000 repeated samples with replacement from the respective zero-truncated sampling (surface) distributions (see Table 3). The sampling surface distributions are exactly the same for attributes length and density under DLS and DLMCS, the differences below arise from different Monte Carlo draws.

Attribute/protocol	Sample size (*m*)					
	10	20	30	50	100	250
Volume (m^3)						
DLS	92.8	93.6	94.6	94.2	94.9	95.5
Sausage	93.0	93.8	93.1	94.8	95.0	95.9
DLMCS	94.7	93.9	94.9	94.4	94.8	94.4
PDS	62.7	85.4	76.6	85.0	91.2	91.8
Length (m)						
DLS	56.8	79.5	91.8	93.1	90.2	94.4
Sausage	92.6	91.9	92.2	93.6	94.0	95.0
DLMCS	58.8	81.9	93.3	91.3	91.6	94.1
PDS	74.0	78.0	79.4	85.1	86.5	91.7
Density						
DLS	88.6	89.5	91.5	90.2	92.8	95.2
Sausage	91.7	94.3	93.1	94.0	92.3	94.9
DLMCS	87.8	90.4	92.0	93.3	93.5	94.1
PDS	78.4	83.5	82.5	86.2	87.7	90.5
Coverage area (m^2)						
DLS	94.2	93.8	95.4	94.4	95.2	96.4
Sausage	93.3	94.4	94.5	95.7	94.3	95.0
DLMCS	95.0	94.3	95.2	95.3	94.9	94.1
PDS	88.6	88.9	89.9	92.4	91.3	93.9

Therefore, for every inclusion zone that overlaps a grid point in the sampling surface, the surface will heap in multiples of 100, generating the trimodal sampling distribution shown in Fig. 5. In addition, the average confidence interval width for PDS was on the order of one-third the width of the other methods for all sample sizes. This all results in the slow convergence to the nominal coverage level seen in the distribution of sample means from this particular log population.

Results for the other attributes are equally interesting and varied. The results for length may require in excess of $m = 100$ sample points for nominal coverage rates. Again, we see that for the distance limited methods a constant amount is accrued for each log at a given point (grid cell), yielding a multimodal sampling distribution, smaller confidence interval widths on average, and hence requiring a larger number of samples. And this is a direct consequence of the method being optimized for length. The sausage method is slightly better because even though it is a probability proportional to length method, the surface accrual is not in constant steps, as can be seen by the inclusion area, a_s, when combined with the general HT estimator (2) (Gove and Van Deusen, 2011). The distribution for PDS is severely negative exponential with a long tail of large values as discussed above, contributing to its poor performance. The results for density are similar to those for length, except that the sampling distributions for the two distance limited methods are strongly exponential in this case. Finally, the sampling distributions for coverage area are quite well behaved for the length-based methods, requiring only $10 \leqslant m \leqslant 20$ sample points for interval estimation. PDS again has a moderate exponential distribution and would require a sizable sampling effort. However, an alternative is to use PDS optimized for coverage area (Ducey et al., 2008), which may produce better results.

4. Discussion

This paper has introduced a new sampling method based on the concept of limiting the distance from an object within which it can be sampled by a random point. This limiting distance concept itself is not new; for example, fixed-area plot protocols do the same thing (Gove and Van Deusen, 2011), and as has been shown, the new sampling protocol is closely related to the sausage sampling protocol for fixed area plots. Both are probability proportional to length methods and both use a fixed distance limit, resulting in an inclusion zone whose area is proportional to log length, leading to different sized zones for each log. Both methods also share a simple measurement protocol based on HT estimation. However, two points differentiate the new distance limited protocol from the sausage protocol. First, there is the obvious difference in the shape of the inclusion zones due to the ability to sample the log from the ends as well as the sides in the sausage protocol (Fig. 2). In the distance limited methods one must be perpendicular to the log 'needle' to even consider whether the log might be a candidate for sampling. The restriction on the distance limited method may seem overly constraining at first glance; however, the original motivation for the method derived from the DLMCS estimator protocol that enables the design-unbiased estimation of all attributes, and this is where the restriction becomes necessary. This latter point forms the second difference, as none of the fixed-area protocols has a Monte Carlo variant.

The field measurement protocols were shown to differ very little in the simulation experiments reported on the estimators. However, there are some subtleties that may make more of a difference in the choice of the two protocols than simply how they are implemented in the field. We have seen (Table 1) that for some attributes such as length and density, the estimators for DLS and DLMCS will be the same. However, for other attributes such as coverage area, volume, or related quantities, there is a difference in the two measurement protocol estimators. For example, under DLS volume would normally be estimated using a model like Smalian's formula. This is contrast with the estimate of volume under DLMCS, which derives from taking a random cross-sectional measurement on a perpendicular from the sample point to the log's needle. As pointed out by Affleck (2008), the former imparts an unknowable model bias, while the latter can produce a more variable estimate, depending on the taper distribution in the log population. In the case of a population of logs that taper dramatically this could impart a high degree of variability in the estimate. However, in the results of the simulations conducted here, using a variety of taper models, the difference between the two protocols in terms of average confidence interval width was negligible for all attributes and all six sample sizes considered in Table 4. This is also supported by the overall sampling surface results in Table 3, where the variability between the two protocols were quite comparable. Therefore, the concern for extra variability in the Monte Carlo protocol under DLS appears unwarranted. But keep in mind that this is a limited study, and field results could be more in line with the above observations, especially when considering log decay and deflation as components of measurement error in either protocol.

In field applications a number of issues can hamper the proper measurement of diameters and cross-sectional areas on down logs, including curved or branched pieces, and decay induced deflation. The former has been addressed in detail by Williams et al. (2005) and Valentine et al. (2001). The field protocols these authors described are appropriate for minimizing measurement error under both distance limited sampling protocols. Unfortunately, the measurement of pieces where deflation has changed the shape of the log itself can be more problematic. This affects all methods for sampling down material, not just those described here, and at present there is no recommended general approach available to the problem beyond ad hoc corrections based on decay classes. However, because the CMC approach does not depend on a solid geometric model in the case of volume estimation, it may accrue less overall error because of the reliance on only diameter-based measurements. Note that if the estimation of carbon content or biomass is desired, then the Monte Carlo sampling point l_j along

Table 5
Surface standard deviation for various distance limits (D_l); the number of grid cells, m_e, falling within the inclusion zones for each level of D_l is also shown based on the population of logs in Table 3.

Attribute/protocol	Distance limit D_l (m)				
	2.5	3	5	8	10
DLS					
Volume (m^3)	48.5	44.4	34.8	28.0	25.1
Length (m)	735.1	674.0	538.6	440.0	394.3
Density	166.8	153.1	121.7	98.4	88.2
Coverage (m^2)	185.6	170.2	134.3	108.9	97.7
DLMCS					
Volume (m^3)	49.2	45.1	35.4	28.6	25.6
Length (m)	735.1	674.0	538.6	440.0	394.3
Density	166.8	153.1	121.7	98.4	88.2
Coverage (m^2)	187.1	171.4	135.2	109.9	98.5
m_e	4893	5755	8811	12696	15146

the log can be used to extract a woody sample for an estimate of bulk density, for example (Valentine et al., 2001).

Only one distance limit was investigated in detail here, therefore it is reasonable to inquire how the results for the two distance limited protocols will change as D_l increases. Obviously an increase in D_l will increase the inclusion zone area for each log. As a result, there will be more overlap between zones, and more logs sampled at each grid cell (sample point). As a rule, as each inclusion zone area increases, the attribute density will be spread out over a larger area. However, the height of the surface within any given inclusion zone depends on $z = \frac{|A|}{2D_l}$, which is a fixed amount for given D_l. Therefore, as D_l increases, z decreases and so the height will decrease for both DLS and DLMCS sampling protocols. This results in a decrease in surface variability for any attribute (Table 5). In general then, it may seem like the larger D_l is, the better. But it is well-known under search based techniques such as PDS, that the larger the K_{pds} factor (and hence the larger the inclusion zone), the more searching is necessary to determine candidate logs, and the higher the probability of missing pieces in the survey. Therefore, there is always an optimal search distance that will minimize possible non-detection bias, while also reducing the variance of the estimate. The best way to determine this in practice is with a small reconnaissance inventory as these factors depend on the population under consideration. Finally, the results in Table 5 show that the two sampling protocols, DLS and DLMCS are consistently comparable in terms of variability of the estimators for any given distance limit tested.

Restricting D_l to a distance that is manageable considering the conditions of the tract to be inventoried in terms of visibility is a strong point for the method. Of the methods compared here, fixed area plots (i.e., the sausage method) allows this same capability as previously mentioned. However, in general there is no design-unbiased estimator for all the usual attributes of interest under fixed-area plot sampling. In contrast, the DLMCS protocol provides the estimator (11), which is design-unbiased for all attributes in Table 1. Similarly, PDS and its extensions (Ducey et al., 2008) also provide design-unbiased estimators. However, because the inclusion zone under PDS depends on a function of diameter, it can be difficult to control the width of the zones such that the search distance does not get too large, unless one has some idea of the maximum log diameter on the tract. Recently, a new PDS variant has been developed that incorporates the distance limited protocols described here to remedy this perceived shortcoming in PDS (Ducey et al., in press). Additionally, PDS requires a distance check that depends on diameter whenever a sample point lies near the boundary of the inclusion zone, necessitating a look-up table of "limiting distances" by diameter. While these are only minor nuisances, having just one limiting distance to worry about, D_l, seems like an potentially attractive alternative.

As discussed in the opening, there are many methods now available for sampling down coarse woody debris. Many comparisons among these methods have been made in the literature, using LIS as a standard. LIS was not used here as a standard for two reasons. First, it has been shown by Williams and Gove (2003) using a similar simulation approach, that overall PDS had lower variance for volume and density estimation than LIS. Secondly, in order to equalize the inclusion zone areas among the different methods compared, a line length of approximately $2D_l$ would be used (it would vary somewhat because the angular differences in line-log intersections result in non-rectangular inclusion zones). This is obviously much shorter than what is normally used in an LIS inventory and therefore unrealistic in general.

The results from the Monte Carlo confidence interval coverage experiments showed a large degree of variability in terms of required sample sizes both by method and attribute (Table 4). It must be emphasized again that these results are applicable to the log population used in the simulations, and potentially to other larger populations with similar sampling distributions. The results should not be taken as a fixed set of guidelines to be appropriated to a given method or attribute for any population. Populations of logs can be constructed that will give quite different sampling distributions, and hence quite different appropriate sample sizes for nominal normal theory coverage (e.g., Gove et al. (in press)), underscoring the difficulty involved in constructing general guidelines applicable to diverse populations.

In the simulations a buffer was created that was large enough so that no part of any log's inclusion zone fell outside the tract boundary, eliminating any requirement for extra boundary overlap correction (Fig. 2). This is essentially what has become known as Masuyama's (Masuyama, 1953; Masuyama, 1954) method, where an external buffer is set up around the tract in which sample points may fall, and still sample logs within the tract. This buffering method may be used in field applications where it is possible to establish such an encompassing zone. In cases where access outside the tract is not possible, one can use a method such as the 'walkthrough' (Ducey et al., 2004). When applying the walkthrough, it is important that any portions of logs extending past the tract boundary be truncated at the boundary and not considered part of the population. Then, one simply applies the walkthrough method by traversing the shortest straight-line distance to the tract boundary, with reference distance taken directly through the log's 'needle' (other walkthrough protocols can also be envisioned). Other related methods have been developed in recent years based on buffering including the 'toss-back' method (Iles, 2003, p. 641), and a set of iterated correction procedures (Holt, 2012). These methods also present unbiased alternatives for boundary correction. A discussion of comparative merits of each is beyond the scope of this paper, interested readers may consult (Ducey et al., 2004), Iles (2003, Chapter 14) and Gregoire and Valentine (2008, §7.5 and 10.7) for a review of these methods.

5. Conclusions

A new method for sampling down coarse woody debris has been presented along with two estimators, one of which (DLMCS) provides design-unbiased estimates for all attributes of interest that can be approximated with integral quantities on the log. Both protocols performed well in comparison to existing methods (fixed-area plot and PDS) that are both similar operationally and in their respective estimation strategies. It appears that field implementation of the distance limited methods based on limited trials is simple and straightforward. The DLMCS protocol should offer no new field-related problems over PDS, which has been thoroughly field tested; and the DLS protocol is familiar to all

who have used fixed-area plots. Finally, like PDS, distance limited sampling could be applied to populations of objects other than logs, providing one can define a suitable 'needle' axis for the object.

Acknowledgements

The authors thank the two anonymous reviewers for their very helpful comments on the manuscript.

References

Affleck, D.L.R., 2008. A line intersect distance sampling strategy for downed wood inventory. Canadian Journal of Forest Research 38, 2262–2273.
Barrett, J.P., Goldsmith, L., 1976. When is *n* sufficiently large? The American Statistician 30, 67–68.
Barrett, J.P., Nutt, M.E., 1979. Survey Sampling in the Environmental Sciences: A Computer Approach. COMPress, Inc.
Bebber, D.P., Thomas, S.C., 2003. Prism sweeps for coarse woody debris. Canadian Journal of Forest Research 33, 1737–1743.
Bowman, J., Sleep, D., Forbes, G., Edwards, M., 2000. The association of small mammals with coarse woody debris at log and stand scales. Forest Ecology and Management 129, 119–124.
Bunnell, F., Houde, I., 2010. Down wood and biodiversity – implications to forest practices. Environmental Reviews 18, 397–421.
Ducey, M.J., Gove, J.H., Valentine, H.T., 2004. A walkthrough solution to the boundary overlap problem. Forest Science 50 (4), 427–435.
Ducey, M.J., Williams, M.S., Gove, J.H., Roberge, S., Kenning, R.S., in press. Distance limited perpendicular distance sampling for coarse woody material: theory and field results. Forestry.
Ducey, M.J., Williams, M.S., Gove, J.H., Valentine, H.T., 2008. Simultaneous unbiased estimates of multiple downed wood attributes in perpendicular distance sampling. Canadian Journal of Forest Research 38, 2044–2051.
Fraver, S., Ringvall, A., Jonsson, B.G., 2007. Refining volume estimates of down woody debris. Canadian Journal of Forest Research 37, 627–633.
Gove, J.H., in press. sampSurf: Sampling Surface Simulation. <https://r-forge.r-project.org/projects/sampsurf/>.
Gove, J.H., Ducey, M.J., Valentine, H.T., Williams, M.S., 2012. A comprehensive comparison of the perpendicular distance method for sampling downed coarse woody debris. Forestry.
Gove, J.H., Ringvall, A., Ståhl, G., Ducey, M.J., 1999. Point relascope sampling of downed coarse woody debris. Canadian Journal of Forest Research 29 (11), 1718–1726.
Gove, J.H., Van Deusen, P.C., 2011. On fixed area plot sampling for downed coarse woody debris. Forestry 84 (2), 109–117.
Gove, J.H., Williams, M.S., Ståhl, G., Ducey, M.J., 2005. Critical point relascope sampling for unbiased volume estimation of downed coarse woody debris. Forestry 78, 417–431.
Gregoire, T.G., Valentine, H.T., 2008. Sampling Strategies for Natural Resources and the Environment. Applied Environmental Statistics. Chapman & Hall/CRC, NY.
Harmon, M., Franklin, J., 1989. Tree seedlings on logs in Picea–Tsuga forests of oregon and washington. Ecology 70, 48–59.
Holt, J.J., 2012. Interating Masuyma's method to reduce sampling variation. Environmental and Ecological Statistics 19, 95–106.
Iles, K., 2003. A Sampler of Inventory Topics, first ed. Kim Iles and Associates.
Masuyama, M., 1953. A rapid method of estimating basal area in timber survey—an application of integral geometry to areal sampling problems. Sankhyā 12 (3), 291–302.
Masuyama, M., 1954. On the error in crop cutting experiment due to the bias on the border of the grid. Sankhyā 14, 181–186.
Pouska, V., Svoboda, M., A, L., 2010. The diversity of wood-decaying fungi in relation to changing site conditions in an old-growth mountain spruce forest, central europe. European Journal of Forest Research 129, 219–231.
R Development Core Team, 2012. R: A Language and Environment for Statistical Computing. R Foundation for Statistical Computing, Vienna, Austria, ISBN: 3-900051-07-0. <http://www.R-project.org>.
Rubinstein, R.Y., Kroese, D.P., 2008. Simulation and the Monte Carlo Method, second ed. John Wiley and Sons.
Ståhl, G., 1998. Transect relascope sampling—a method for the quantification of coarse woody debris. Forest Science 44 (1), 58–63.
Ståhl, G., Gove, J.H., Williams, M.S., Ducey, M.J., 2010. Critical length sampling: a method to estimate the volume of downed coarse woody debris. European Journal of Forest Research 129, 993–1000.
Suess, E.A., Trumbo, B.E., 2010. Introduction to Probability Simulation and Gibbs Sampling with R. Springer.
Thompson, S.K., 1992. Sampling. John Wiley & Sons, NY.
Valentine, H.T., Gove, J.H., Ducey, M.J., Gregoire, T.G., Williams, M.S., 2008. Estimating the carbon in coarse woody debris with perpendicular distance sampling. In: Hoover, C.M. (Ed.), Field Measurements for Forest Carbon Monitoring: A Landscape-Scale Approach. Springer, NY, pp. 73–87.
Valentine, H.T., Gove, J.H., Gregoire, T.G., 2001. Monte Carlo approaches to sampling forested tracts with lines or points. Canadian Journal of Forest Research 31, 1410–1424.
Van Deusen, P., 1990. Critical height versus importance sampling for log volume: does critical height prevail? Forest Science 36 (4), 930–938.
van Wagner, C.E., 1968. The line intersect method in forest fuels sampling. Forest Science 14, 267–276.
Warren, W.G., Olsen, P.F., 1964. A line intersect method for assessing logging waste. Forest Science 3, 267–276.
Williams, M.S., 2001a. New approach to areal sampling in ecological surveys. Forest Ecology and Management 154, 11–22.
Williams, M.S., 2001b. Nonuniform random sampling: an alternative method of variance reduction for forest surveys. Canadian Journal of Forest Research 31, 2080–2088.
Williams, M.S., Gove, J.H., 2003. Perpendicular distance sampling: an alternative method for sampling downed coarse woody debris. Canadian Journal of Forest Research 33, 1564–1579.
Williams, M.S., Valentine, H.T., Gove, J.H., Ducey, M.J., 2005. Additional results for perpendicular distance sampling. Canadian Journal of Forest Research 35, 961–966.
Woodall, C.W., Heath, L.S., Smith, J.E., 2008. National inventories of down and dead woody material forest carbon stocks in the United States: challenges and opportunities. Forest Ecology and Management 256, 221–228.
Woodall, C.W., Rondeux, J., Verkerk, P.J., Ståhl, G., 2009. Estimating dead wood during national forest inventories: a review of inventory methodologies and suggestions for harmonization. Environmental Management 44, 624–631.